Atomic L-Shell Coster-Kronig, Auger, and Radiative Rates and Flourescence Yields for Na-Th†

Eugene J. McGuire
Sandia Laboratories, Albuquerque, New Mexico 87115
(Received 21 August 1970)

Calculated Auger, Coster-Kronig, and radiative transition rates are used to compute atomic L-shell Coster-Kronig and fluorescence yields. The results are compared with other calculations, experimental yield determinations, and radiative half-width measurements.

I. INTRODUCTION

This is the third of a series of papers on atomic fluorescence yields. The first two[1] treated transitions arising from an initial K-shell hole and outlined the calculational procedures. The K-shell calculations stopped at $Z = 54$, where relativistic effects begin to appear, since these are nonrelativistic calculations. These L-shell calculations are carried out to $Z = 90$. At $Z = 90$, the L_1 ionization energy is roughly half that of the K shell at $Z = 54$. While this is no guarantee that nonrelativistic L-shell calculations are valid at $Z = 90$, there is no good counterargument, calculational and experimental, that such nonrelativistic calculations are invalid. Such evidence may appear in a comparison with experiment of calculated nonrelativistic L-shell Auger[2] and Coster-Kronig[3] term intensities. This

TABLE I. Total radiative rates for L-shell holes, in 10^{-4}/a.u. (1 a.u. = 2.42×10^{-17} sec). The direct calculations are labeled "model," while "adj" refers to the model results adjusted to the observed energy difference of the $L_1 - M_{2,3}$, $L_2 - M_4$, and $L_3 - M_{4,5}$ transitions. Scof refers to Scofield's calculations (Ref. 11).

	L_1			L_2			L_3		
Z	Model	Adj	Scof	Model	Adj	Scof	Model	Adj	Scof
11				0.00023	0.00023		0.00023	0.00023	
12				0.00089	0.00089		0.00089	0.00089	
13	0.0016	0.0016		0.0027	0.0027		0.0027	0.0027	
14	0.0063	0.0063		0.0029	0.0029		0.0029	0.0029	
15	0.017	0.017		0.0044	0.0044		0.0044	0.0044	
16	0.036	0.036		0.0061	0.0061		0.0061	0.0061	
17	0.067	0.067		0.0085	0.0085		0.0085	0.0085	
18	0.124	0.124		0.0116	0.0116		0.0116	0.0116	
19	0.172	0.172		0.0165	0.0165		0.0165	0.0165	
20	0.234	0.234		0.0230	0.016		0.0230	0.015	
22	0.40	0.40		0.144	0.112		0.144	0.104	
24	0.65	0.64		0.469	0.42		0.469	0.40	
26	1.12	1.08		1.08	0.93		1.08	0.86	
28	1.41	1.46		1.74	1.86		1.74	1.73	
30	1.93	1.92		3.14	3.40		3.14	3.20	
32	3.18	3.00		5.39	5.40		5.39	5.05	
34	4.65	4.82		6.80	7.60		6.80	7.00	
36	6.42	6.50	6.18	9.84	10.0	9.08	9.84	9.60	8.86
38	9.04	9.40		13.2	11.8		13.2	11.0	
40	12.1	12.2	11.5	19.4	19.7	17.4	19.4	16.0	16.8
42	16.7	17.2	15.1	25.8	26.4	23.5	25.8	23.7	22.6
44	21.2	23.0		31.9	34.6		31.9	31.0	
47	27.3	34.0	28.0	43.6	52.0	46.1	43.6	47.0	44.0
50	41.2	50.0	39.2	63.1	72.0	65.7	63.1	62.5	61.4
54	66.2	88		97.9	117		97.9	96.0	
60	104	133	104	157	203	176	157	170	164
67	178	245		278	370		278	290	
74	290	440	296	438	625	514	438	460	457
79	453	615	411	713	900	721	713	625	631
83	480	820		727	1200		727	795	
90	727	1480	897	1123	2200	1577	1123	1180	1188

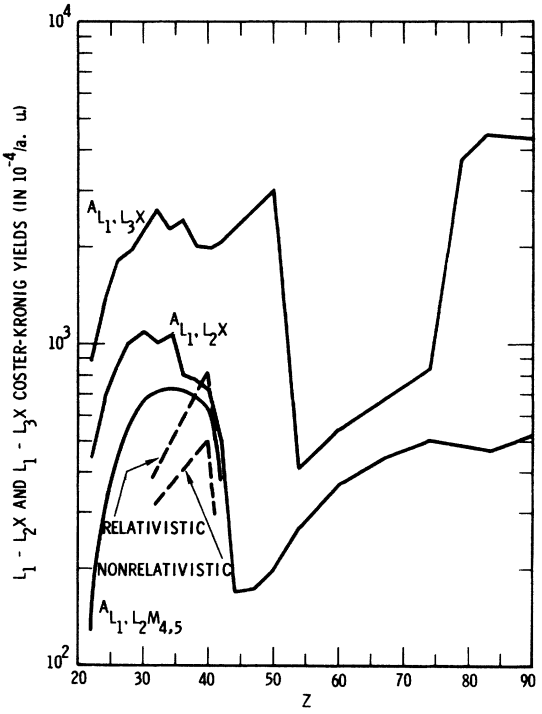

FIG. 1. Total L_1-shell Coster-Kronig transition rates and $L_1-L_2M_{4,5}$ rate. The solid figures are our calculations; the dashed figures are from Ref. 12. The units are 10^{-4}/a.u. (1 a.u. = 2.42 $\times 10^{-17}$ sec.).

is presently being done.[4]

In Sec. II we discuss the formal expressions used and procedures invoked to adjust the calculated rates to the observed energy values. In Sec. III we compare the adjusted calculations with experiment, and in Sec. IV we compare our calculations with some radiative half-width measurements.

II. CALCULATED TRANSITION RATES

The Auger total rates were calculated in LS coupling (the total Auger rates are independent of coupling). Expressions for the total rates in LS coupling for an initial s, p, or d hole and final combinations of s, p, and d holes can be found in a report of the author.[5] Asaad[6] has obtained expressions for term intensities in j-j coupling for an initial s or p hole and final combinations of s, p, and d holes. These expressions were used in computing Coster-Kronig rates. However, neither Refs. 5 or 6 contain expressions for transitions involving final f holes. Both total Auger rates in LS coupling and expressions for term intensities in j-j coupling for transitions involving final-state f holes have been obtained by the author.[7]

In the Auger process with an initial nl hole, and final $n'l'$ and $n''l''$ holes, we have used[1] $|E_{nl}-E_{n'l'}-E_{n''l''}|$ as the energy of the electron in the continuum. The E_{nl} values are one-electron eigenvalues obtained from our approximation to the central potential of Herman and Skillman.[8] In the K-shell calculations and in the L-shell Auger and radiative rate calculations, we adjust the calculated rates to experimental energy values by the following procedure: The rates calculated in our model are plotted as a function of the model energy difference of a prominent transition, i.e., $L_{\rm I}$-$M_{2,3}$, $L_{\rm II}$-M_4, and $L_{\rm III}$-$M_{4,5}$. Then the adjusted value is obtained by using the measured energy difference[9] for the prominent transition.

However, in Coster-Kronig transitions, n' or $n''=n$ so that the continuum electron has a small energy and the transition probability can be enormous. If the energy difference is negative, the transition does not occur. The one-electron eigenvalues calculated from a central potential of the Herman and Skillman type are crude. Comparison of Coster-Kronig energies calculated in this way, with those obtained from the ESCA tabulation[10] show wide differences. The Coster-Kronig energy differences formed from the ESCA ionization thresholds are not the experimental energy differences (if these were available) but are undoubtedly closer to the correct values than those obtained from the Herman and Skillman approach. This is seen in comparing experimental Auger transition energies with energy differences formed with the two sets of ionization thresholds. Thus we use the ESCA energy differences in the Coster-Kronig transition rates only.

The central potentials used were those of Herman and Skillman with a $2s$ hole. The one-electron eigenvalues showed small differences when a $2p$ hole was used instead of a $2s$ hole, but these differences were much less than those arising from our straight-line approximation[1] to either central potential.

In Table I we list the radiative transition rates obtained with the straight-line approximation, the adjusted radiative rates, and the relativistic calculations of Scofield[11] for Z values where we overlap. It can be seen that the model radiative rates are in general within 10% of Scofield's value and that, except for $L_{\rm III}$, the adjusted radiative rates are in poorer agreement with Scofield's values. Scofield's calculations are based on a relativistic version of the central potential of Herman and Skillman, and include retardation. Our calculations are nonrelativistic, in LS coupling, using the dipole approximation. At $Z=90$, with a $2s$ hole, the Herman-Skillman $2s$-$3p$ and $2p$-$3d$ eigenvalue differences are 946 and 945 Ry, respectively. With our approximation, the differences are 903 and 936 Ry, respectively. The experimental L_1-M_2, L_1-M_3, L_2-M_4, L_3-M_4, and L_3-M_5 energy differences are 1150, 1207, 1191, 941, and 953 Ry, respectively.

TABLE II. L_1 Auger transition rates for various shell combinations in 10^{-4}/a.u. (1 a.u. = 2.42×10^{-17} sec). "Tot" refers to the direct calculation of the total Auger transition rate and "Adj tot" to model results adjusted to experimental energy differences.

Z	L_1MM	L_1NN	L_1OO	L_1MN	L_1MO	L_1NO	Tot	Adj tot
12	3.88						3.88	3.88
13	9.19						9.19	9.19
14	16.3						16.3	16.3
15	23.0						23.0	23.0
16	31.4						31.4	31.4
17	42.8						42.8	42.8
18	51.1						51.1	51.1
19	55.0			2.48			57.5	57.5
20	61.5	0.065		5.79			67.4	67.4
22	75.3	0.080		6.87			82.3	82.3
24	97.0			5.66			103	102
26	124	0.050		7.77			132	128
28	155	0.041		7.59			163	166
30	186	0.036		8.20			194	197
32	226	0.20		13.3			239	240
34	281	0.44		18.7			300	297
36	263	0.76		25.5			289	291
38	289	0.97	0.002	29.8	2.28	0.15	322	322
40	295	1.44	0.002	38.5	2.70	0.18	338	344
42	340	2.45		58.4	1.25	0.12	402	414
44	383	3.42		70.4	1.08	0.14	458	463
47	380	5.50		89.5	1.04	0.15	476	505
50	414	8.15	0.015	110.3	5.05	0.87	538	583
54	491	10.7	0.078	142.5	12.4	1.78	658	735
60	543	13.7	0.134	153.7	14.9	2.60	728	740
67	526	15.6	0.109	186.7	13.2	2.47	744	820
74	600	18.3	0.190	225.6	19.5	3.87	868	920
79	649	18.0	0.340	222.7	30.6	4.85	925	990
83	615	23.7	0.50	257.0	34.7	6.63	937	1060
90	648	27.0	0.89	297.2	50.7	9.63	1033	1200

Not unexpectedly, for the L_3 radiative transition rate, where the model and experimental energy differences are close, the model, adjusted and Scofield rate are in agreement (< 5% difference). Significant differences occur when the model and experimental energy differences are not close. It appears that Scofield's[11] correction procedure somehow accounts for the experimental energy difference directly in the radiative matrix element. Our correction procedure is outlined above. The correct radiative rates for high Z are thus open to question. We have calculated the various yields using both the adjusted radiative rates and Scofield's. They are shown in Sec. III.

In Fig. 1 we show the calculated L_I Coster-Kronig total transition rates A_{L_1,L_2X} and A_{L_1,L_3X} and the partial rate $A_{L_1,L_2M_{4,5}}$. Also shown are the calculated relativistic and nonrelativistic $A_{L_1,L_2M_{4,5}}$ rates of Talukdar and Chattarji.[12] They find a significant difference between the relativistic and nonrelativistic results. However, they use screened hydrogenic wave functions[13] which proved inaccurate for K-shell Auger calculations,[1] and which should, in general, be even less accurate for both Coster-Kronig transitions (since the continuum orbital has an energy much less than in Auger transitions) and for L-shell transitions (since internal and external screening are more important than in the K-shell case). Further, the relativistic results of Talukdar and Chattarji are considerably larger than their nonrelativistic results but our nonrelativistic results are, in general, larger than their relativistic calculations. It appears that the use of screened hydrogenic wave functions precludes any conclusions on the importance of relativistic effects in L-shell Coster-Kronig yields.

The large drops in the computed rates after $Z = 42$ for A_{L_1,L_2X} and after $Z = 50$ for $A_{L_1L_3X}$ is due to the energetics which forbid L_1-$L_2M_{4,5}$ transitions. After $Z = 74$ the energetics again allows L_1-$L_3M_{4,5}$ transitions, accounting for the sharp rise in $A_{L_1L_3X}$.

All the matrix elements used in the calculations are available from the author.[14] In Table II we list the L_1 Auger rates for transitions arising from

TABLE III. $L_{2,3}$ Auger transition rates for various shell combinations, total Auger rates, adjusted total Auger rates, and Coster-Kronig rates, all in 10^{-4}/a.u. (1 a.u. $= 2.42 \times 10^{-17}$ sec.).

Z	$L_{23}MM$	$L_{23}NN$	$L_{23}OO$	$L_{23}MN$	$L_{23}MO$	$L_{23}NO$	Tot	Adj tot L_{II}	Adj tot L_{III}	L_2, L_3X
12	0.26						0.26	0.26		
13	1.81						1.81	1.81		
14	6.48						6.48	6.48		
15	13.6						13.6	13.6		
16	25.1						25.1	25.1		
17	41.6						41.6	41.6		
18	61.5						61.5	61.5		
19	68.5			0.64			69.1	69.1		
20	78.2	0.008		1.60			79.8	75.0	73.0	
22	94.2	0.008		1.92			96.1	88.5	88.4	
24	127.1			0.65			128	124	121	
26	166.5	0.006		1.48			168	157	153	
28	214	0.005		1.39			215	223	214	
30	281	0.004		1.29			282	284	292	
32	353	0.005		6.96			360	355	346	
34	385	0.28		17.3			402	388	386	
36	396	0.84		28.8			426	403	398	40.7
38	436	1.35	0.0002	38.2	0.28	0.031	476	455	441	60.5
40	501	2.50	0.0003	64.3	0.30	0.049	568	572	526	79.0
42	551	3.00		76.0	0.17	0.016	630	634	612	93.2
44	571	4.45		88.4	0.18	0.017	664	680	658	112
47	585	8.06		136.3	0.15	0.016	730	753	734	145
50	606	11.6	0.005	165.5	2.81	0.41	786	822	786	178
54	671	15.3	0.079	201.3	11.3	1.66	901	944	894	222
60	790	19.5	0.141	248.3	16.6	2.77	1078	1110	1088	215
67	814	23.7	0.112	281.2	14.6	3.99	1137	1205	1150	252
74	872	28.8	0.246	318	25.0	4.64	1249	1285	1255	269
79	912	23.7	0.384	307	37.7	7.34	1288	1290	1285	334
83	813	31.0	0.624	330	48.3	8.75	1232	1390	1250	291
90	854	35.7	1.33	391	73.1	13.6	1369	1535	1380	426

various shell combinations, the total Auger rate, and the adjusted total Auger rate. In Table III we list the L_2 and L_3 Auger rates as above and also the Coster-Kronig L_2, L_3X rates. The L_2, L_3X rate jumps between $Z = 83$ and $Z = 90$ since at $Z = 90$ the energetics allow a L_2, L_3M_5 transition.

III. YIELDS

In Table IV we list the fluorescence yields (ω) and Coster-Kronig yields (f_{ij}). For an L_3 hole there is no Coster-Kronig yield and the measurements are unambiguous. In Fig. 2 we compare the calculated ω_3 with experimental values. Below $Z = 65$ the measured values are ω_{KL}, an average of ω_2 and ω_3 measured following a $2p$-$1s$ radiative transition filling a K-shell hole. In this region the difference between computed ω_2 and ω_3 values is less than the error quoted in ω_{KL}. The ω_{KL} values are taken from the review article of Fink *et al.*,[15] except for values at $Z = 38$ and 47 taken from Bailey and Swedlund.[16] Above $Z = 65$ the ω_3 values are from Jopson *et al.*[17] for $Z = 67$, 68, and 70, Holmes and Kostroun[18] for $Z = 67$ and 68, Mohan *et al.*[19] at $Z = 70$, Rao and Crasemann[20] at $Z = 73$ and 80, Palms *et al.*[21] at $Z = 80$, Rao *et al.*[22] at $Z = 82$, Freund and Fink[23] at $Z = 83$, and the remainder from Price *et al.*[24] Agreement between calculation and experiment is seen to be excellent. However, there appears to be a significant variation in measured ω_3 values dependent on the technique used to make the L_3 hole. At $Z = 80$ Rao and Crasemann[20] measure $\omega_3 = 0.40 \pm 0.02$, when the L_3 hole occurs due to a radiative transition following ionization of the K shell by an external x-ray beam. Palms *et al.*[21] measure $\omega_3 = 0.30 \pm 0.01$ at $Z = 80$, when the K electron is removed in the nuclear decay of ^{198}Au and ^{204}Tl. The calculated value is $\omega_3 = 0.34$. Since our adjusted radiative yields do not differ from Scofield's for L_3, there is no difference in the two sets of ω_3 values.

A direct measurement of total fluorescence radiation following creation of an L_2 hole measures $\nu_2 = \omega_2 + f_{23}\omega_3$. Without a measurement of f_{23} one cannot determine ω_2. In Fig. 3 we compare the calculated ν_2 values with the measurements of Refs. 17–24. Again the measured values of ν_2 following

TABLE IV. Coster-Kronig and fluorescence yields for $13 \leq Z \leq 90$. (The notation 3.05-6 means 3.05×10^{-6}.)

Z	$f_{1,2}$	$f_{1,3}$	$f_{1,2}+f_{1,3}$	ω_1	$f_{2,3}$	ω_2	ω_3
13			0.982	3.05-6			0.002 40
14			0.975	9.77-6			0.001 08
15			0.971	2.12-5			4.1-4
16			0.968	3.63-5			2.9-4
17			0.964	5.60-5			2.3-4
18			0.965	8.58-5			1.9-4
19			0.962	1.15-4			2.1-4
20			0.955	1.56-4			2.1-4
22	0.313	0.629	0.942	2.80-4			0.001 18
24	0.317	0.636	0.953	2.97-4			0.003 29
26	0.302	0.652	0.954	3.84-4			0.005 59
28	0.325	0.622	0.947	4.63-4			0.008 02
30	0.322	0.624	0.946	5.23-4			0.010 8
32	0.266	0.671	0.938	7.70-4			0.014 4
34	0.302	0.616	0.918	0.001 30			0.017 8
36	0.230	0.686	0.915	0.001 85	0.0897	0.0220	0.023 6
38	0.249	0.646	0.894	0.003 00	0.115	0.0224	0.024 3
40	0.236	0.648	0.884	0.003 97	0.118	0.0294	0.029 5
42	0.166	0.689	0.856	0.005 75	0.124	0.0350	0.037 3
44	0.057	0.779	0.836	0.007 74	0.136	0.0418	0.045 0
47	0.052	0.786	0.838	0.010 2	0.152	0.0547	0.060 2
50	0.052	0.784	0.835	0.013 0	0.162	0.0656	0.073 7
54	0.179	0.274	0.454	0.058 4	0.173	0.0912	0.097 0
60	0.207	0.303	0.510	0.074 6	0.141	0.133	0.135
67	0.202	0.309	0.511	0.112	0.138	0.203	0.201
74	0.195	0.332	0.527	0.115	0.123	0.287	0.268
79	0.083	0.644	0.727	0.105	0.132	0.357	0.327
83	0.069	0.656	0.735	0.120	0.101	0.417	0.389
90	0.069	0.575	0.644	0.197	0.102	0.529	0.461

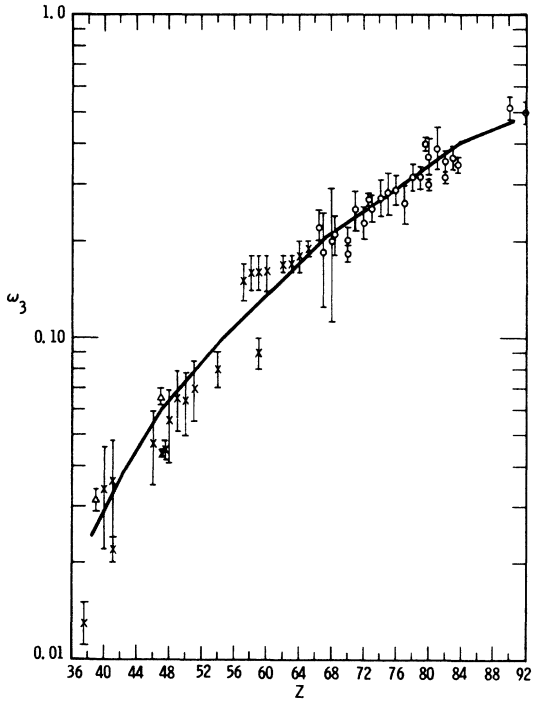

FIG. 2. Fluorescence yield ω_3. The solid curve connects our calculated values. The experimental data are from Refs. 15–24.

nuclear conversion are lower than those following external ionization of the K shell, especially at $Z = 70$ and 83. Figure 4 compares the calculated f_{23} values with five recent measurements.[19–22] Again at $Z = 80$, two measurements, one using nuclear conversion, the other external ionization, to produce the initial K-shell hole, lead to significantly different results. The open circles in Fig. 4 are computed f_{23} values using our Coster-Kronig and adjusted Auger yields and Scofield's[11] radiative yields. Clearly the choice of radiative rates leads to no more than a 20% difference. Because of the limited data and large error bars in experimental f_{23} values we do not compare calculated and experimental ω_2 values. For ω_2 the largest change in computed value due to the two sets of radiative yields is 15% at $Z = 90$. Finally, from Table IV it can be seen that for $Z \geq 67$ our calculations predict $\omega_2 > \omega_3$. But for $Z = 83$ Freund and Fink report $\omega_2 = 0.23 \pm 0.02$ and $\omega_3 = 0.345 \pm 0.018$.

In Fig. 5 we show calculated and measured ω_1 and ν_1 values, where $\nu_1 = \omega_1 + f_{12}\omega_2 + (f_{13} + f_{12}f_{23})\omega_3$. The measured values are from Refs. 15, 22, and 23. The open circles are again calculations with Scofield's radiative yields. In Fig. 6 we show computed and measured f_{12} and f_{23} values. The open circles are values computed with Scofield's radia-

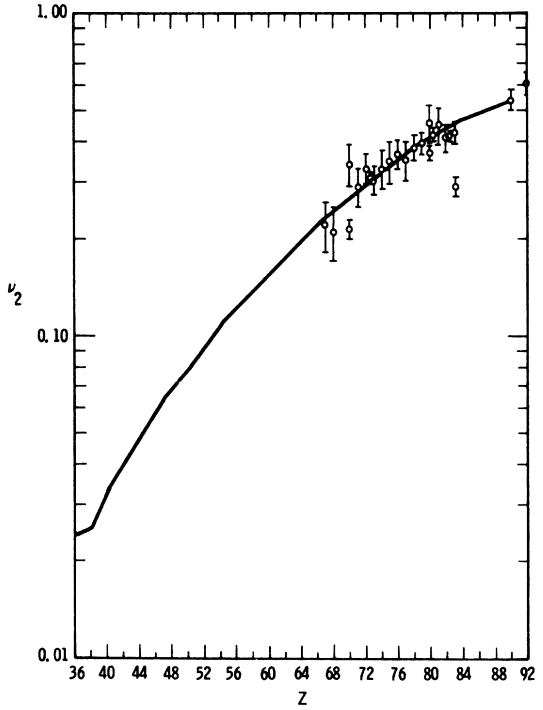

FIG. 3. Fluorescence yield ν_2. The solid curve connects our calculated values. The experimental data is from Refs. 16–24. The open circles are recent measurements of ω_3, the crosses are older measurements of ω_{KL}, and the triangles are recent measurements of ω_{KL} from Ref. 16.

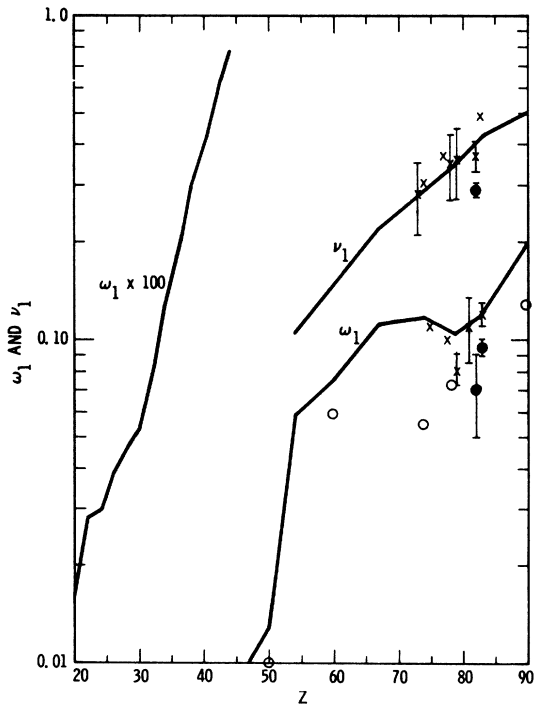

FIG. 5. L_1 radiative yields ω_1 and ν_1. The solid curves connect our calculated values. The open circles arise from using Scofield's (Ref. 11) radiative rates in place of ours. The experimental values are from Refs. 15, 22, and 23.

tive rates.

Finally, from the yields from various shell combinations, one can compute the number of M holes arising from the decay of an L hole, $n_{L,M}$. These results are shown in Table V. At $Z = 83$, Freund and Fink[25] find $n_{L_1,M} = 1.77$ and $n_{L_3,M} = 1.36$ while we find 1.78 and 1.33, respectively. But they find $n_{L_2,M} = 1.44$ while we find 1.29. However, we have already mentioned their anomalous[24] ω_2 value at $Z = 83$. This may account for the difference.

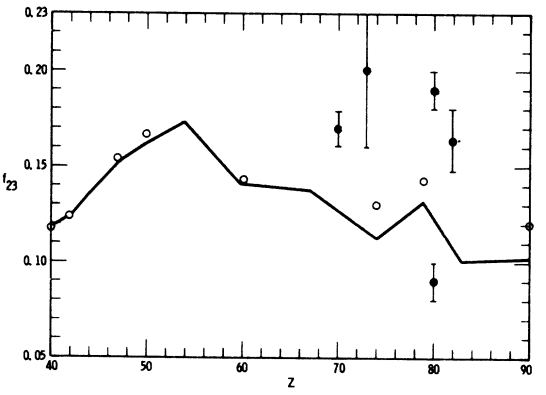

FIG. 4. Coster-Kronig yield $f_{2,3}$. The solid curve connects our calculated values. The open circles arise from using Scofield's (Ref. 11) radiative rates in place of ours. The experimental values are from Refs. 19–23.

IV. RADIATIVE HALF-WIDTHS

The half-width in an nl-$n'l'$ radiative transition is related to the total decay rates by

$$\Delta E = \hbar(A^{nl}_{\text{tot}} + A^{n'l'}_{\text{tot}}) \ .$$

Half-widths for the $K\alpha_1$ and $K\alpha_2$ lines have long been known from experiment.[26,27] If the total K-shell transition rate were known, the $K\alpha_1$ and $K\alpha_2$ half-widths could be used to determine the total L_3 and L_2 transition rates. Scofield has computed the

TABLE V. Calculated average number of M-shell holes arising from the decay of an L-shell hole.

Z	$^nL_1, M$	$^nL_2, M$	$^nL_3, M$
50	2.34	1.67	1.69
54	1.59	1.63	1.64
60	1.58	1.59	1.60
67	1.46	1.51	1.53
74	1.93	1.43	1.45
79	1.92	1.36	1.38
83	1.78	1.29	1.33
90	1.61	1.22	1.23

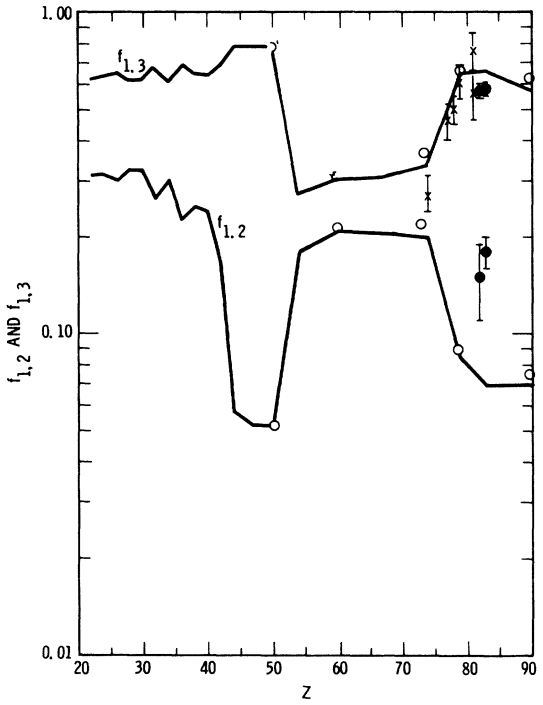

FIG. 6. L_1-shell Coster-Kronig yields $f_{1,2}$ and $f_{1,3}$. The solid curves connect our calculated values. The open circles arise from using Scofield's (Ref. 11) radiative rates in place of ours. The experimental values are from Refs. 15, 22, and 23.

total radiative rate for a K-shell hole. Since for $Z \gtrsim 65$, the K-shell fluorescence yield ω_K is almost unity, the radiative yield is approximately the total yield. We have used the measured half-widths of Nelson *et al.*[27] and Scofield's[11] radiative yields to determine the L_3 and L_2 total yields (in eV). They are shown in Table VI, with our computed half-widths. Agreement is generally poor. However, Nelson *et al.* estimate their half-width measurements are accurate to ± 10%. Subtracting Scofield's radiative yields leads to values about 25% of the half-width. Thus, while the error bars should be large in the derived L_3 and L_2 total transition rates, this will not account for the large discrepancies seen in Table VI.

TABLE VI. Total transition rate for L_2 and L_3 holes in eV. Derived results are obtained from the measurements of Nelson *et al.* (Ref. 27) and Scofield's (Ref. 11) calculations; computed results are our adjusted total transition rates.

	Derived		Computed	
Z	$A_{L_2}^{Tot}$	$A_{L_3}^{Tot}$	$A_{L_2}^{Tot}$	$A_{L_3}^{Tot}$
65	6.9	7.7		
67			4.95	3.90
70	7.0	11.8		
74	8.8	11.1	5.91	4.65
79	12.1	6.5	6.84	5.18
82	16.6	20.6		
83			7.81	5.54
90	11.5	11.2	11.3	6.94

V. CONCLUSIONS

The limited amount of experimental data on L-shell yields, and the discrepancies seen in the measurements, make it premature to comment on the validity of these calculations. On the whole, the calculations are in good agreement with the present experimental data, though measurements with smaller error bars may modify this. Clearly, measurements should be done for $Z < 70$ and on $L\alpha$, $L\beta$, and $L\gamma$ radiative half-widths. Clearly too, calculations should be made on detailed Auger and Coster-Kronig term intensities, and these are under way.

†Work supported by the U.S. Atomic Energy Commission.

[1]E. J. McGuire, Phys. Rev. 185, 1 (1969); Phys. Rev. A 2, 273 (1970).
[2]P. Auger, J. Phys. Radium 6, 205 (1925).
[3]D. Coster and R. Kronig, Physica 2, 13 (1935).
[4]E. J. McGuire, Phys. Rev. (to be published).
[5]E. J. McGuire, Sandia Laboratories Research Report No. SC-RR-69-137 (unpublished).
[6]W. N. Asaad, Nucl. Phys. 44, 415 (1963).
[7]E. J. McGuire, Sandia Laboratories Research Report No. SC-RR-70-429 (unpublished).
[8]F. Herman and S. Skillman, *Atomic Structure Calculations* (Prentice-Hall, Englewood Cliffs, N. J., 1963).
[9]J. A. Bearden, Rev. Mod. Phys. 39, 78 (1967).
[10]K. Siegbahn *et al.*, in *ESCA, Atomic, Molecular and Solid State Structure Studied by Means of Electron Spectroscopy* (Nova Acta Regiae Societatis Upsaliensis, Uppsala, 1967), Ser. IV, Vol. 20.
[11]J. H. Scofield, Phys. Rev. 179, 9 (1969).
[12]B. Talukdar and D. Chattarji, Phys. Rev. A 1, 33 (1970).
[13]E. J. Callen, Phys. Rev. 124, 793 (1961).
[14]E. J. McGuire, Sandia Laboratories Research Report No. SC-RR-70-558 (unpublished).
[15]R. W. Fink, R. C. Jopson, H. Mark, and C. D. Swift, Rev. Mod. Phys. 38, 513 (1966).
[16]L. E. Bailey and S. B. Swedlund, Phys. Rev. 158, 6 (1967).
[17]R. C. Jopson, J. M. Khan, C. D. Swift, and M. A. Williamson, Phys. Rev. 131, 1165 (1963).
[18]C. P. Holmes and V. O. Kostroun, Bull. Am. Phys. Soc. 15, 561 (1970).
[19]S. Mohan, H. O. Freund, R. W. Fink, and P. Venugopala Rao, Phys. Rev. C 1, 254 (1970).
[20]P. Venugopala Rao and B. Crasemann, Phys. Rev. 139, A1926 (1965).
[21]J. M. Palms, R. E. Wood, P. Venugopala Rao, and V. O. Kostroun, Phys. Rev. C 2, 592 (1970).
[22]P. Venugopala Rao, R. E. Wood, J. M. Palms, and R. W. Fink, Phys. Rev. 178, 1997 (1969).

[23]H. U. Freund and R. W. Fink, Phys. Rev. 178 1952 (1969).
[24]R. E. Price, H. Mark, and C. D. Swift, Phys. Rev. 176, 3 (1968).
[25]H. U. Freund and R. W. Fink, Phys. Rev. 183, 1055 (1969).
[26]S. K, Allison, Phys. Rev. 44, 63 (1933).
[27]G. C. Nelson, W. John, and B. G. Saunders, Phys. Rev. 187, 1 (1969).

PHYSICAL REVIEW A VOLUME 3, NUMBER 2 FEBRUARY 1971

Quantum Mechanics of a Double Perturbation: Application to the Zeeman Effect of Metastable Hydrogen Molecules*

William Lichten†
New Haven Public Schools,† New Haven, Connecticut 06520
(Received 10 August 1970)

A general theorem is derived which applies to any quantum-mechanical system subject to two perturbations H and G. It is shown that the eigenvalues of the system can be found by first solving exactly the secular equation in H. Then the first-order perturbation of the energy by G can be written explicitlv without solving for the eigenfunctions. This leads to a simple method for finding the exact Landé g factors for the Zeeman effect of any quantum-mechanical system. These results are applied to the Zeeman effect of the hydrogen molecule in the metastable $c^3\pi_u$ state. Jette and Cahill's theory of the Zeeman effect is extended to cover all magnetic fields. Excellent agreement is found between experimental g factors and theory. At higher magnetic fields, "anti-crossings" are found between pairs of states for which $\Delta J = \pm 1, \pm 2$, $\Delta F = 0, \pm 1, \pm 2$, and $\Delta M_F = 0$. The repulsion between these levels is very small, of the order of a few Mc/sec. This causes the noncrossing rule of von Neumann and Wigner to be violated experimentally. The Landau-Zener theory of level crossings is applied. It is shown that the observed loss of quantization in the molecular-beam experiments is consistent with theory.

I. INTRODUCTION AND HISTORICAL SUMMARY

This paper is concerned with perturbation theory, which is commonly applied to the problem of magnetism in atoms, molecules, nuclei, and solids. Although the lodestone was known to the ancient world, Michael Faraday[1] was the first man to observe and distinguish the two forms of diamagnetism and paramagnetism. Maxwell's macroscopic equations for the electric and magnetic fields were extended to the microscopic world by Lorentz.[2] Classical electron theory predicted the effect of the surrounding media on the internal electric and magnetic fields of atoms or molecules.[2,3]

The advent of the precise molecular-beam magnetic-resonance experiments by Rabi and co-workers[4] made it necessary to consider the magnetic field produced within an atom by its own diamagnetism. Lamb[5] derived an expression for the diamagnetic shielding in spherically symmetric atoms. The paramagnetic nuclear or electronic moment of an atom interacts so as to produce an energy which is linearly dependent on the external field:

$$E = -\vec{\mu} \cdot \vec{B}. \tag{1}$$

The diamagnetic interaction produces an additional field which is linearly dependent on the external magnetic vector:

$$\vec{B} = \vec{B}_{ext} + \vec{B}_{int} = (1 - \sigma)\vec{B}, \tag{2}$$

which effectively reduces the paramagnetic moment by the shielding factor σ. Equivalently, the internal paramagnetic moment produces a polarization of the diamagnetic charge cloud, which interacts with the external field to produce the same result as in Eq. (2). Lamb calculated the shielding factor to be $\sigma = 0.319 \times 10^{-4}\, Z^{4/3}$, on the basis of the Fermi-Thomas atom model, which gives a shift normally a small fraction of a percent.

The nuclear-magnetic-resonance technique, invented by Bloch *et al.* and Purcell *et al.*,[6] opened the way to observing the nuclear coupling with external fields in a wide variety of chemical surroundings. Soon it was found that the shielding factor of (2) varied from one molecule to another. Ramsey[7] developed an extension of Van Vleck's theory of magnetism[3] to explain the "chemical shift." He pointed out that the shift can be large when a paramagnetic state is nearby to perturb the diamagnetic state in question.

At that time, Kusch[8] found a discrepancy of about 0.7% between the magnetic moments of Ga isotopes as measured in nuclear magnetic resonances and molecular-beam experiments, which were done on atoms in the paramagnetic ^2P states. Foley[9] showed that this discrepancy was caused by a partial break-